Materials Research Letters

ISSN: (Print) 2166-3831 (Online) Journal homepage: https://www.tandfonline.com/loi/tmrl20

Impact of TiO_2-II phase stabilized in anatase matrix by high-pressure torsion on electrocatalytic hydrogen production

Kaveh Edalati, Qing Wang, Hiroto Eguchi, Hadi Razavi-Khosroshahi, Hoda Emami, Miho Yamauchi, Masayoshi Fuji & Zenji Horita

To cite this article: Kaveh Edalati, Qing Wang, Hiroto Eguchi, Hadi Razavi-Khosroshahi, Hoda Emami, Miho Yamauchi, Masayoshi Fuji & Zenji Horita (2019) Impact of TiO_2-II phase stabilized in anatase matrix by high-pressure torsion on electrocatalytic hydrogen production, Materials Research Letters, 7:8, 334-339, DOI: 10.1080/21663831.2019.1609111

To link to this article: https://doi.org/10.1080/21663831.2019.1609111

MATER. RES. LETT.
2019, VOL. 7, NO. 8, 334–339
https://doi.org/10.1080/21663831.2019.1609111

MATERIALS RESEARCH LETTERS
Taylor & Francis
Taylor & Francis Group

ORIGINAL REPORT

Impact of TiO_2-II phase stabilized in anatase matrix by high-pressure torsion on electrocatalytic hydrogen production

Kaveh Edalati[a,b], Qing Wang[a], Hiroto Eguchi[a,c], Hadi Razavi-Khosroshahi[d], Hoda Emami[a], Miho Yamauchi[a,c], Masayoshi Fuji[d] and Zenji Horita[a,b]

[a]WPI, International Institute for Carbon-Neutral Energy Research (WPI-I2CNER), Kyushu University, Fukuoka, Japan; [b]Department of Materials Science and Engineering, Faculty of Engineering, Kyushu University, Fukuoka, Japan; [c]Department of Applied Chemistry, Faculty of Engineering, Kyushu University, Fukuoka, Japan; [d]Advanced Ceramics Research Center, Nagoya Institute of Technology, Gifu, Japan

ABSTRACT

Electrocatalysis using renewable energy sources provides a clean technology to produce hydrogen from water. Titanium oxide is considered as a potential electrocatalyst not only for hydrogen production but also for CO_2 conversion. In this study, to enhance the cathodic electrocatalytic activity of TiO_2, the phase composition on TiO_2 surface is modified by inclusion of high-pressure TiO_2-II phase using high-pressure torsion (HPT) straining. Detailed spectroscopic studies revealed that the energy band gap is reduced and the valence band energy increased with increasing the TiO_2-II fraction. The highest electrocatalytic activity for hydrogen production was achieved on an anatase-rich nanocomposite containing TiO_2-II nanograins.

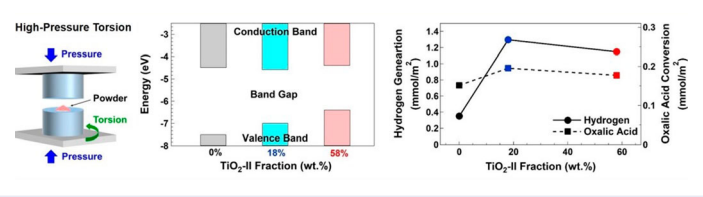

IMPACT STATEMENT

The first application of high-pressure TiO_2-II phase for electrocatalysis confirm that the inclusion of phase in anatase-based nanocomposites is effective to enhance the electrocatalytic hydrogen production on titanium oxide due to the modification of electronic structure.

ARTICLE HISTORY
Received 18 December 2018

KEYWORDS
Severe plastic deformation (SPD); titanium dioxide (TiO_2); TiO_2-II columbite phase; electrocatalysis; water splitting

Hydrogen is considered as a clean energy carrier for future energy-storage applications, but production of hydrogen without emitting CO_2 is still challenging [1]. Photocatalytic water splitting is an ideal technique to produce hydrogen [2], but the technique is not sufficiently effective for the mass production of hydrogen yet [3]. Electrocatalytic hydrogen production from water splitting by using renewable energy sources (i.e. power to gas conversion) is regarded as a main strategy to store renewable energies in the form of hydrogen gas [4]. Electrocatalysis is also widely used for converting undesirable compounds to useful materials such as conversion of CO_2 to fuels [5].

TiO_2 is one of the most investigated electrocatalysts due to its environmental-friendly features, stability and low cost, but its electrocatalytic activity needs to be improved [6]. So far, different techniques such as doping [7], addition of metallic particles [8], formation of hybrid structures containing organic or carbon-based materials [9] and fabrication of hetrostructures containing two polymorphs [10,11] have been employed to enhance the electrocatalytic activity of TiO_2. Among these techniques, the formation of structures with different phases is the only strategy that is applicable to TiO_2 in the pure form and thus it is the most environmental-friendly technique.

CONTACT Kaveh Edalati kaveh.edalati@kyudai.jp WPI, International Institute for Carbon-Neutral Energy Research (WPI-I2CNER), Kyushu University, Fukuoka 819-0395, Japan; Department of Materials Science and Engineering, Faculty of Engineering, Kyushu University, Fukuoka 819-0395, Japan; Qing Wang wangqing@i2cner.kyushu-u.ac.jp WPI, International Institute for Carbon-Neutral Energy Research (WPI-I2CNER), Kyushu University, Fukuoka 819-0395, Japan

Supplemental data for this article can be accessed here. https://doi.org/10.1080/21663831.2019.1609111

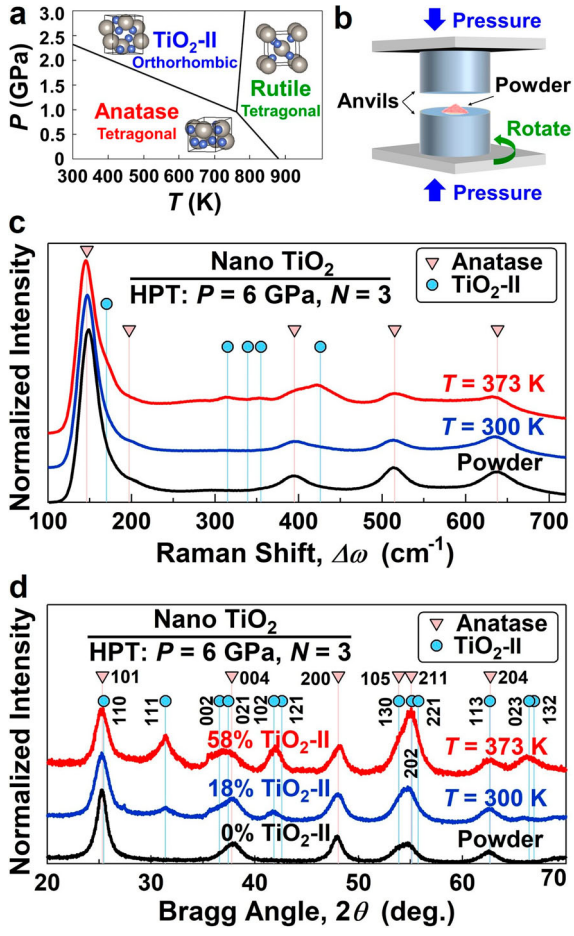

Figure 1. TiO_2-II phase formation by HPT processing. (a) Pressure-temperature phase diagram of TiO_2; (b) principles of HPT; (c) Raman spectra and (d) XRD profiles for TiO_2 samples before and after HPT processing at 300 and 373 K. Reference XRD data for anatase and TiO_2-II phases were taken from JCPDS card numbers of 01-071-1166 and 01-084-1750, respectively, for atomic planes with relative intensities higher than 9%.

As shown in Figure 1(a), TiO_2 has several phases such as rutile and anatase with the tetragonal structure and TiO_2-II (columbite) with the orthorhombic structure [12]. Although anatase exhibits the best catalytic activity due to its large specific surface area [6], it was shown that the two-phase structure of rutile in anatase-rich matrix can exhibit better activity for both photocatalytic activity [13] and electrocatalytic activity [10]. Such an improvement was attributed to the interphase effect on charge separation and increasing the electron/hole recombination time [14,15]. A recent study showed that the high-pressure TiO_2-II phase can exhibit a low band gap and enhanced photocatalytic activity for water splitting [16] in agreement with the predictions of density functional theory calculations [17]. Although the TiO_2-II phase can be synthesized by different methods such as high-pressure high-temperature process [12], hydrothermal compression [18], high-pressure torsion (HPT) method [16,19], thin film deposition [20,21] and chemical reaction [22], there have been no reports on the electrocatalytic activity of TiO_2-II.

In this study, we report the first application of TiO_2-II phase as an electrocatalyst for not only hydrogen production from water but also for hydrogenation of oxalic acid to produce an alcoholic compound. It should be noted that the group of authors recently reported the electrochemical hydrogenation of oxalic acid (divalent carboxylic acid) to produce glycolic acid (monovalent alcoholic compound) and found that the catalytic activity on TiO_2 considerably depends on the crystal structure, i.e. anatase exhibits extremely high reducibility for oxalic acid but rutile does not [23,24]. The difference in catalytic activity was attributed to the reducibility of electrons introduced from electrode to the conduction band bottom of TiO_2, i.e. electrons accumulated in the conduction band of anatase are located at energy levels higher than those of rutile one [25]. Here, to examine the electrocatalytic activity of TiO_2-II phase, the phase is stabilized by HPT [26,27], a method which showed high potential for stabilizing high-pressure phases in different metallic and non-metallic systems [28,29]. Interestingly, TiO_2-II possesses a narrow band gap compared to that for anatase TiO_2, which means that the conduction band bottom or valence band top of TiO_2-II is located at the position different from that of anatase TiO_2. Here, we first examine the effect of TiO_2-II on energy states and subsequently apply the TiO_2-II mixed catalysts to electrochemical reduction of water and oxalic acid. It is found that the presence of TiO_2-II in anatase can enhance the electrocatalytic activity.

For experiments, commercially pure anatase (ST-01) powder with ~7 nm crystallite size was processed by HPT under 6 GPa for 3 turns at room temperature (300 K) and 373 K with a rotation speed of 1 rpm. The HPT-processed samples, which were in the form of discs with 10 mm diameter and ~0.8 mm thickness, were examined at 2–5 mm away from the disc center (i.e. in highly strained regions) by different techniques.

First, the phase transformation was analyzed by X-ray diffraction (XRD) using Cu Kα radiation and by Raman spectroscopy using 532 nm laser.

Second, microstructure of samples was examined by Cs-corrected high-resolution transmission electron microscopy (TEM) using an acceleration voltage of 200 kV.

Third, the bandgap and electronic structure of samples were examined by ultraviolet–visible light diffuse reflectance (UV–VIS) spectroscopy, X-ray photoelectron spectroscopy (XPS) using Al Kα radiation and ultraviolet photoelectron spectroscopy (UPS) using a He discharge lamp.

Fourth, the electrocatalytic activity for electrochemical reductions of water and oxalic acid were examined. 10 mg of TiO_2 samples were crushed and dispersed in 0.2 mL ethanol and deposited on two sides of Ti foils with the dimensions of $25 \times 20 \times 0.1$ mm^3. The foils were further calcinated at 473 K for 1 h to achieve good bonding between the foil and the TiO_2 particles (TiO_2-II remains stable at this temperature [16]). A three-electrode system (TiO_2 on Ti foil as cathode, Pt spiral wire as anode and Ag/AgCl as reference) and two sealed cells separated by a Nafion membrane were used for the electrocatalytic reactions. For water splitting, the electrolytes in both anodic and cathodic cells were a solution of 0.2 M Na_2SO_4 with a PH of 6.85. For oxalic acid decomposition, the electrolyte was a mixture of 0.2 M Na_2SO_4 and 0.03 M oxalic acid in the cathodic cell and 0.2 M Na_2SO_4 with a PH of 2.1 in the anodic cell (PH was adjusted by addition of H_2SO_4). After setting the system, the electrodes were connected to a potentiostat and the cathodic cells were bubbled by N_2 or Ar for 30 min to remove the air. The electrocatalytic tests were conducted for 30 min at 298 K with −1.65 V versus reversible hydrogen electrode for water splitting and at 323 K with –0.7 V versus reversible hydrogen electrode for oxalic acid conversion. The reaction products were analyzed by gas chromatography for water splitting and by liquid chromatography for oxalic acid decomposition.

The occurrence of phase transformation is confirmed using the Raman spectra and XRD profiles, as shown in Figure 1(b,c), respectively. While only anatase peaks are visible in the intial powder, the peaks of TiO_2-II appear after HPT processing at 300 K and these peak intensities increase with increasing the processing temperature to 373 K. Detailed analysis using the Rietveld method confirms that the fraction of TiO_2-II is 18 and 58 wt% after HPT processing at 300 and 373 K, respectively. The formation of TiO_2-II phase after HPT processing is consistent with earlier publications [16,19], but the fraction of TiO_2-II phase after HPT processing at 300 K is lower in this study compared to earlier publications due to the small crystallite size of starting powder which can inhibit the phase transformation [30]. However, the fraction of TiO_2-II increases by processing at 373 K due to the reduction of energy barrier for phase transformation [12]. Selected area electron diffraction analysis, as shown in supporting Fig. S1, also confirms the formation of TiO_2-II phase after HPT processing with the lattice planes consistent with the XRD analysis.

The presence of nanograins of anatase in the initial powder and the formation of nanograins of TiO_2-II after HPT processing are visible in high-resolution TEM images of Figure 2. The initial powder has an average grain size of 7 ± 2 nm and the average grain size

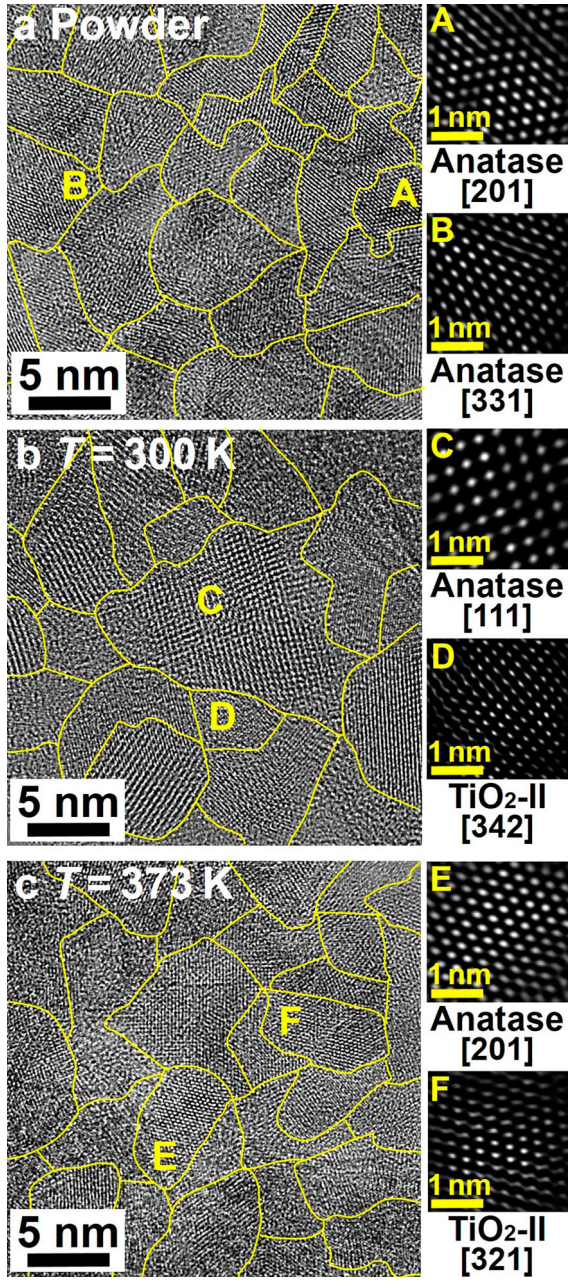

Figure 2. Coexistence of nanograined TiO_2-II and anatase phases after HPT processing. TEM micrographs (left) and lattice images corresponding to grains A–F (right) for (a) TiO_2 powder and for samples processed by HPT at (b) 300 K and (c) 373 K.

remains unchanged after HPT processing, i.e. 7 ± 2 nm and 7 ± 3 nm after processing at 300 and 373 K, respectively. The main change after HPT processing is the presence of TiO_2-II, as confirmed by fast Fourier transform (FFT) diffractograms and shown in lattice images of Figure 2 by inverse FFT. It should be noted that the HPT processing usually results in grain refinement in various metals [27,31] and non-metallic materials [19,32], but the absence of grain refinement is this study is a natural consequence of small grain sizes of initial powder.

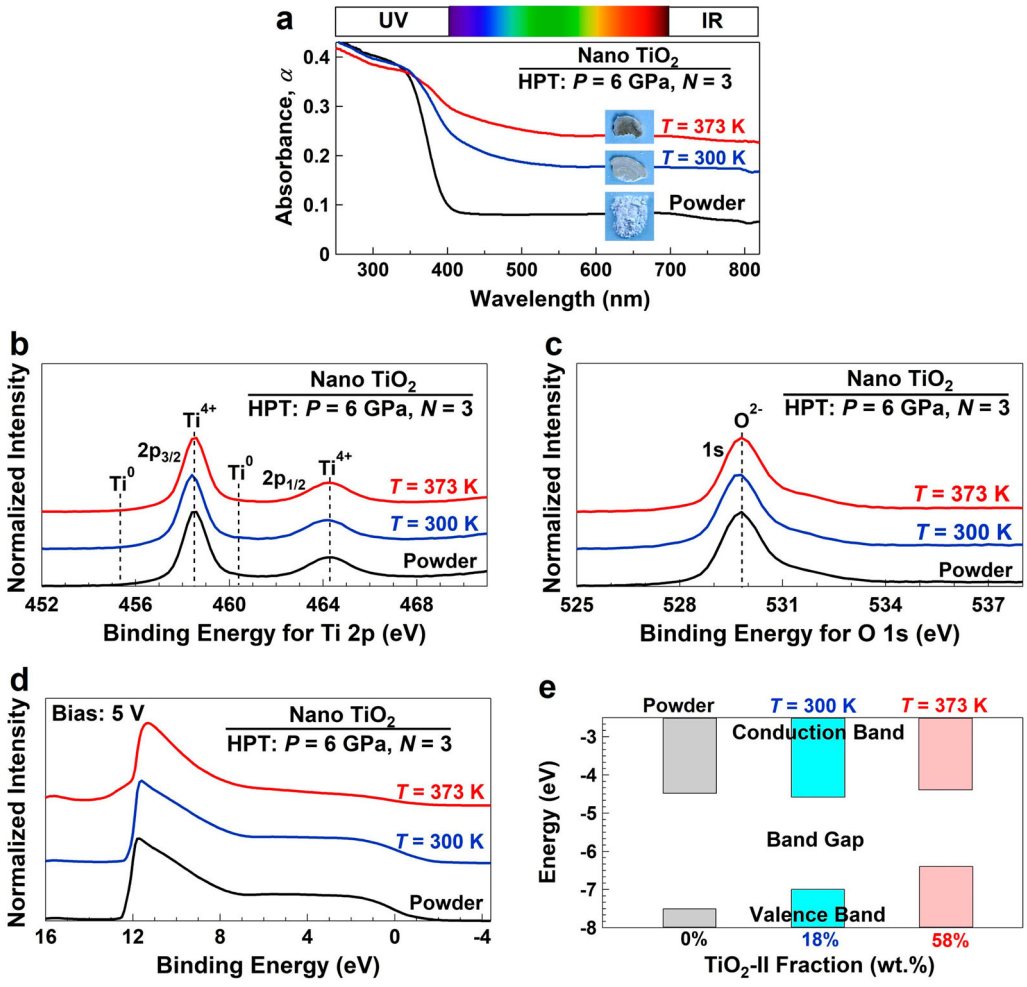

Figure 3. Band gap narrowing and enhancement of valence band energy by TiO_2-II formation via HPT process. (a) UV–VIS diffused reflectance, (b) XPS Ti 2p, (c) XPS O 1s and (d) UPS spectra together with (e) variations of valence band and conduction band energies for TiO_2 samples before and after HPT processing at 300 and 373 K. Inset in (a): appearance of samples.

The influence of HPT processing and the resultant formation of TiO_2-II on electronic structure of TiO_2 was investigated by UV–VIS spectroscopy, XPS and UPS as shown in Figure 3. UV–VIS spectra show that the light absorbance increases by HPT processing and by increasing the processing temperature, indicating that the band gap narrowing occurs by the TiO_2-II formation in good agreement with the earlier reports on the formation of TiO_2-II by HPT [16] or by thin film deposition [20]. Evaluation of UV–VIS data using the Kubelka–Munk analysis [33] shows that the optical band gap is 3.0, 2.4 and 2.0 eV for the initial powder and for the samples processed by HPT at 300 and 373 K, respectively. It should be noted that the color of samples changes from white to gray and dark gray as shown in Figure 3(a), indicating that oxygen vacancies should have formed during HPT processing. However, the concentration of vacancies should be minor as no XPS Ti 2p and O 1s peak shifts are visible in Figure 3(b,c), respectively. Combination of UPS and UV–VIS spectroscopy using the procedure described in [34] can elucidate the effect of TiO_2-II fraction on the electronic structure of the two-phase TiO_2 composites. As shown in Figure 3(e), the valence band energy of the three samples increases by HPT processing, whereas the conduction band energy does not change significantly. The band gap decreases and the valence band energy increases by increasing the fraction of TiO_2-II phase, which is beneficial for electrocatalysis as will be discussed below.

Influence of the TiO_2-II formation on electrocatalytic activity per unit mass of TiO_2 is shown in Figure 4(a) for hydrogen production and for oxalic acid conversion, which were examined individually. The sample with 18 wt.% TiO_2-II phase shows the highest activity for water splitting, however, the anatase powder shows the best activity for the electrocatalytic reduction of oxalic acid. Since the HPT method partially consolidates the oxide powders and reduces their surface area [35,36],

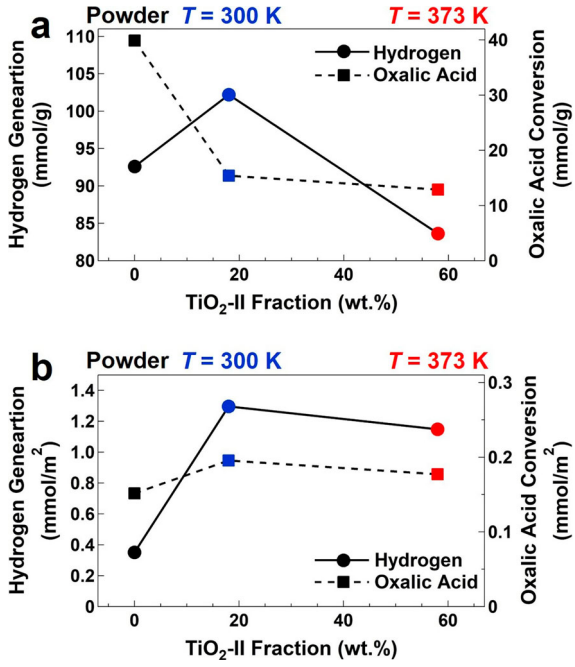

Figure 4. Enhancement of electrocatalytic activity by formation of TiO_2-II phase in anatase matrix. Electrocatalytic hydrogen generation from water and oxalic acid conversion per unit (a) mass and (b) area of TiO_2 for samples before and after HPT processing at 300 and 373 K.

the catalytic activity data in Figure 4(a) are possibly influenced by reduced surface area effect. To examine this effect, surface areas were measured using the Brunauer–Emmett–Teller (BET) method and the electrocatalytic data were plotted per unit area in Figure 4(b). The surface areas were 263, 79 and 73 m^2/g for the initial powder and for the samples processed by HPT at 300 and 373 K, respectively. Figure 4(b) indicates that the amount of hydrogen is considerably enhanced by the inclusion of TiO_2-II grains and the best electrocatalytic activity for hydrogen evolution is achieved on the sample with 18 wt% TiO_2-II, whereas the conversion of oxalic acid on the three TiO_2 catalysts seems almost similar. Considering that the energy position of conduction band bottom predominantly influences the electrocatalytic oxalic acid conversion [23–25], the observed activities on TiO_2 catalysts for oxalic acid conversion are plausible because the conduction band energy levels are reasonably the same for the three samples. Taken altogether, it is concluded that the presence of some amounts of TiO_2-II as the second phase in the anatase matrix can improve the electrocatalytic activity for hydrogen evolution, but the best fraction of TiO_2-II phase for electrocatalytic activity still needs to be optimized in future studies.

A question naturally arises from the current observations: why the anatase-based nanocomposites with 18 wt.% of TiO_2-II exhibits the best electrocatalytic activity for hydrogen evolution among the three selected samples. It was shown broadly that anatase shows better catalytic activity than other polymorphs of TiO_2 such as rutile mainly due to its larger specific surface area at the liquid–solid interfaces [6]. TiO_2-II phase is a high-pressure phase with lower specific surface area than anatase [12], and thus it is expected that this phase shows lower electrocatalytic activity than anatase. However, the presence of TiO_2-II in anatase lowers the band gap and improves the charge conductivity for electrocatalytic activity. Moreover, the presence of TiO_2-II with higher valence band energy than anatase can produce interphase junctions with better charge separation and distribution similar to the anatase-rutile hetrostructures [13–15]. As shown earlier for the anatase-rutile mixtures, anatase should be the dominant phase to achieve enhanced electrocatalytic activity due to the large specific surface area of anatase [10]. Cao *et al.* showed that the presence of rutile nanowires in anatase film improves the photoelectrocatalysis, while the presence of anatase nanowires in the rutile film results in strongly negative performance [10]. The current results confirm that the electrocatalytic activity of anatase is better than TiO_2-II, but addition of some amounts of TiO_2-II with low band gap and high valence band energy can improve the electrocatalytic activity compared to the single-phase anatase catalyst.

In summary, this study introduces a simple method to synthesize anatase-TiO_2-II nanocomposites as potential electrocatalysts for hydrogen production from water. The presence of TiO_2-II phase in these nanocomposites reduces the band gap and increases the valence band energy and subsequently improves the electrocatalytic activity.

Disclosure statement

No potential conflict of interest was reported by the authors.

Funding

This work is supported in part by WPI-I2CNER, Japan, and in part by Grants-in-Aid for Scientific Research from MEXT, Japan [16H04539 and 26220909]. The HPT process was carried out in IRC-GSAM at Kyushu University.

References

[1] Bak T, Nowotny J, Rekas M, et al. Photo-electrochemical hydrogen generation from water using solar energy. materials-related aspects. Int J Hydrogen Energy. 2002; 27:991–1022.

[2] Fujishima A, Honda K. Electrochemical photolysis of water at a semiconductor electrode. Nature. 1972;238: 37–38.

[3] Ohtani B. Photocatalysis A to Z: what we know and what we do not know in a scientific sense. J Photoch Photobio C. 2010;11:157–178.
[4] Sapountzi FM, Gracia JM, Weststrate CJ, et al. Electrocatalysts for the generation of hydrogen, oxygen and synthesis gas. Prog Energ Combust Sci. 2017;58:1–35.
[5] Kuhl KP, Hatsukade T, Cave ER, et al. Electrocatalytic conversion of carbon dioxide to methane and methanol on transition metal surfaces. J Am Chem Soc. 2014;136:14107–14113.
[6] Bourikas K, Kordulis C, Lycourghiotis A. Titanium dioxide (anatase and rutile): surface chemistry, liquid-solid interface chemistry, and scientific synthesis of supported catalysts. Chem Rev. 2014;114:9754–9823.
[7] Karlsson RKB, Cornell A, Pettersson LGM. The electrocatalytic properties of doped TiO_2. Electrochim Acta. 2015;180:514–527.
[8] Danilov FI, Tsurkan AV, Vasileva EA, et al. Electrocatalytic activity of composite Fe/TiO_2 electrodeposits for hydrogen evolution reaction in alkaline solutions. Int J Hydrogen Energy. 2016;41:7363–7372.
[9] Jing L, Yang ZU, Zhao YF, et al. Ternary polyaniline-graphene-TiO_2 hybrid with enhanced activity for visible-light photoelectrocatalytic water oxidation. J Mater Chem A. 2014;2:1068–1075.
[10] Cao F, Xiong J, Wu F, et al. Enhanced photoelectrochemical performance from rationally designed anatase/rutile TiO_2 heterostructures. ACS Appl Mater Inter. 2016;8:12239–12245.
[11] Li X, Yu J, Low J, et al. Engineering heterogeneous semiconductors for solar water splitting. J Mater Chem A. 2015;3:2485–2534.
[12] Dachille F, Simons PY, Roy R. Pressure-temperature studies of anatase, brookite, rutile and TiO_2-II. Am Mineral. 1968;53:1929–1939.
[13] Ohno O, Sarukawa K, Tokieda K, et al. Morphology of a TiO_2 photocatalyst (Degussa P-25) consisting of anatase and rutile crystalline phases. J Catal. 2001;203:82–86.
[14] Zhang J, Xu Q, Feng Z, et al. Importance of the relationship between surface phases and photocatalytic activity of TiO_2. Angew Chem. 2008;120:1790–1793.
[15] Sun X, Dai W, Wu G, et al. Evidence of rutile-to-anatase photo-induced electron transfer in mixed-phase TiO_2 by solid-state NMR spectroscopy. Chem Commun. 2015;51:13779–13782.
[16] Razavi-Khosroshahi H, Edalati K, Hirayama M, et al. Visible-light-driven photocatalytic hydrogen generation on nanosized TiO_2-II stabilized by high-pressure torsion. ACS Catal. 2016;6:5103–5107.
[17] Kuo MY, Chen CL, Hua CY, et al. Density functional theory calculations of dense TiO_2 polymorphs: implication for visible-light-responsive photocatalysts. J Phys Chem B. 2005;109:8693–8700.
[18] Spektor K, Tran DT, Leinenweber K, et al. Transformation of rutile to TiO_2-II in a high pressure hydrothermal environment. J. Solid State Chem. 2013;206:209–216.
[19] Razavi-Khosroshahi H, Edalati K, Arita M, et al. Plastic strain and grain size effect on high-pressure phase transformations in nanostructured TiO_2 ceramics. Scr Mater. 2016;124:59–62.
[20] Das A, Chowdhury BN, Saha R, et al. Ultrathin vapor-liquid-solid grown titanium dioxide-II film on bulk GaAs substrates for advanced metal-oxide-semiconductor device applications. IEEE Trans Electron Dev. 2018;65:1466–1472.
[21] Das A, Chowdhury BN, Saha R, et al. Formation of high-pressure phase of titanium dioxide (TiO_2-II) thin films by vapor-liquid-solid growth process on GaAs substrate. Phys Status Solidi A. 2018:23;1800640.
[22] Grey IE, Li C, Madsen IC, et al. TiO_2-II. Ambient pressure preparation and structure refinement. Mater Res Bull. 1988;23:743–753.
[23] Watanabe R, Yamauchi M, Sadakiyo M, et al. CO_2-free electric power circulation via direct charge and discharge using the glycolic acid/oxalic acid redox couple. Energy Environ Sci. 2015;8:1456–1462.
[24] Yamauchi M, Ozawa N, Kyobo M. Experimental and quantum chemical approaches to develop highly selective nanocatalysts for CO_2-free power circulation. Chem Rec. 2016;16:2249–2259.
[25] Fukushima T, Kitano S, Yamauchi M. Carbon-neutral energy cycles using alcohols. Sci Tech Adv Mater. 2018;19:142–152.
[26] Valiev RZ, Estrin Y, Horita Z, et al. Producing bulk ultrafine-grained materials by severe plastic deformation. JOM. 2006;58(4):33–39.
[27] Zhilyaev AP, Langdon TG. Using high-pressure torsion for metal processing: fundamentals and applications. Prog Mater Sci. 2008;53:893–979.
[28] Edalati K, Horita Z. A review on high-pressure torsion from 1935 to 1988. Mater Sci Eng A. 2016;652:325–352.
[29] Kilmametov AR, Ivanisenko Y, Mazilkin AA, et al. The $\alpha \rightarrow \omega$ and $\beta \rightarrow \omega$ phase transformations in Ti-Fe alloys under high-pressure torsion. Acta Mater. 2018;144:337–351.
[30] Levitas VI, Javanbakht M. Phase transformations in nanograin materials under high pressure and plastic shear: nanoscale mechanisms. Nanoscale. 2014;6:162–166.
[31] Pippan R, Scheriau S, Taylor A, et al. Saturation of fragmentation during severe plastic deformation. Annu Rev Mater Res. 2010;40:319–343.
[32] Edalati K, Arimura M, Ikoma Y, et al. Plastic deformation of $BaTiO_3$ ceramics by high-pressure torsion and changes in phase transformations, optical and dielectric properties. Mater Res Lett. 2015;3:216–221.
[33] Kubelka P, Munk F. An article on optics of paint layers. Zeit Fur Teken Physik. 1931;12:593–601.
[34] Chun WJ, Ishikawa A, Fujisawa H, et al. Conduction and valence band positions of Ta_2O_5, TaON, and Ta_3N_5 by UPS and electrochemical methods. J Phys Chem B. 2003;107:1798–1803.
[35] Edalati K, Horita Z. Application of high-pressure torsion for consolidation of ceramic powders. Scr Mater. 2010;63:174–177.
[36] Edalati K. Review on recent advancements in severe plastic deformation of oxides by high-pressure torsion (HPT). Adv Eng Mater. 2019;21:1800272.